How to Cite:
Mehihi, A. A. R., Kubba, A. A. R., & Tahtamouni, L. H. (2022). Discovery of new fenamate-based derivatives as anticancer agents and potent VEGFR-2 inhibitors: Design, synthesis, and in silico study. *International Journal of Health Sciences*, *6*(S6), 9160–9179. https://doi.org/10.53730/ijhs.v6nS6.12421

Discovery of new fenamate-based derivatives as anticancer agents and potent VEGFR-2 inhibitors: Design, synthesis, and *in silico* study

Abbas A. Ridha Mehihi
Iraqi Ministry of Health, Thi-Qar Health Directorate, Thi-Qar -Iraq
*Corresponding author email: dr_abbas81@yahoo.com

Ammar A. Razzak Kubba
Department of pharmaceutical chemistry, college of Pharmacy-Bab-Almoudam. University of Baghdad, Baghdad,10001-Iraq

Lubna H. Tahtamouni
Department of Biology and Biotechnology, Faculty of Science, The Hashemite University, Zarqa, Jordan | Department of Biochemistry and Molecular Biology, College of Natural Sciences, Colorado State University, Fort Collins, Colorado, USA

Abstract---VEGFR-2 is a critical target for the treatment of solid tumors. This work represents synthetic approaches to a new class of fenamate-based derivatives with essential pharmacophoric properties comparable to VEGFR-2 inhibitors. The reaction of tolfenamic acid hydrazide with substituted phenacyl bromide, and phenylisothiocynate derivatives produced novel tolfenamic acid (TA) derivatives (compounds 4 and 5). The target molecules were validated using spectroscopic techniques such as FT-IR and 1HNMR. Docking tests were performed to determine how the synthesized chemicals bind to the putative molecular target, VEGFR-2. The docking results demonstrated that the synthesized compounds could bind VEGFR-2 correctly. Finally, computational physicochemical analysis of the most active candidates revealed that they have favorable assets and reasonable drug-likeness reports.

Keywords---tolfenamic acid, synthesis, angiogenesis, VEGFR-2 inhibitors, molecular docking.

Highlights

- A new derivatives of the parent molecules (tolfenamic acid) bearing oxadiazole and hydrazine-1-carbothiamide moeities were designed and synthesized.
- *In silico* cytotoxicity evaluation for the synthesized compounds against VEGFR-2 tyrosine kinase.
- Computational physicochemical estimation displayed the synthesized compounds as reasonable drug-likeness agents.
- The results indicated that compound 5 could be introduced as a potent tyrosine inhibitor.

Graphical abstract

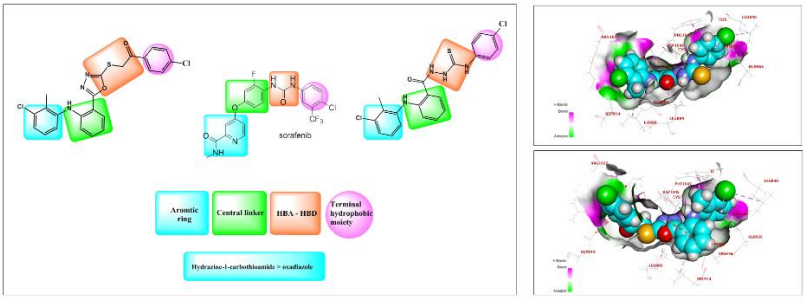

The structure-activity relationship (SAR) of the new compounds and sorafenib revealed several common features.

Introduction

For centuries, cancer has been the most difficult and deadly condition to treat. Worldwide, cancer is the second leading cause of mortality after cardiovascular disease (CVD)[1]. Cancer claimed the lives of 9.6 million people at the end of 2018. The current anticancer therapy has numerous side effects, due to the non-selectivity of drug and drug resistance development. It is still critical to develop novel anticancer medications with minimum to no side effects on healthy cells, in order to inhibit cancer cell multiplication[2]. Protein tyrosine kinases play a crucial role in cell proliferation, migration, survival, and progression at the molecular level of biology. Tyrosine kinases phosphorylate the tyrosine residues in proteins, hence altering their activity. In rare circumstances, tyrosine kinases become permanently activated, resulting in cancer[3]. Tyrosine kinase receptors (RTKs) are a family of cell surface receptors that operate as signaling molecules in response to polypeptides, hormones, and growth factors. Studies have found a large number of receptor tyrosine kinases (RTKs), including vascular endothelial growth factor receptors (VEGFRs), and endothelial growth factor receptors (EGFRs)[4].

Angiogenesis is a multilevel process in which endothelial cells are stimulated, separated, migrated, and multiplied in order to generate new blood vessels out of the ones that are already there. It has been shown to be critical during embryo

development, wound healing, and reproduction[5]. Metastasis of primary tumors is an angiogenesis-dependent process that is regulated by a variety of stimulatory and inhibitory pathways, with growth factors such as VEGF, EGF, FGF, and PIGF being essential regulators. VEGF is a powerful angiogenic tyrosine kinase receptor that is overexpressed in the majority of solid tumors[6]. VEGFR-2 is the primary mediator of VEGF-induced angiogenic signaling, which attracts the target to certain advanced malignancies for involvement in multitier angiogenesis methods such as, vascular permeability, endothelial cell proliferation, migration, and survival[7]. Additionally, sorafenib, sunitinib, axitinib, vatalanib, and regorafenib are examples of the small-molecule VEGFR-2 inhibitors that have been given the go-ahead for usage in clinical trials in the treatment of cancer[8]. Taking these factors into account, targeting VEGFR-2 is a promising technique for achieving quantitative benefit in cancer treatment.

Tyrosine kinase inhibitors, often known as TKIs, are pharmaceutical agents that attach to the ATP binding site on VEGF receptors, and block the kinase activity of the receptors, this method for targeting angiogenesis, which have been shown to be effective in clinical studies and have received official approval for use in clinical practice[9]. As a result, tyrosine kinase inhibitors (TKIs) prevent the phosphorylation of the tyrosine residue, which in turn prevents the transmission of signaling down the intercellular pathway. Sorafenib and sunitinib are considered to be the pioneering representatives of this category of agents[10]. In this study, we aimed to investigate *in silico* cytotoxic and VEGFR-2 inhibiting effects of the prepared (TA) derivatives. The current study employed a strategy to synthesize new tolfenamic acid derivatives, with potential VEGFR-2. inhibitor

Experimental

Materials and Methods

Tolfenamic acid (TA) was bought from China's Hyper Chemical Limited. All chemicals were identified spectroscopically using an IR spectrophotometer (Shimadzu-Japan) in the pharmaceutical chemistry laboratory at the University of Baghdad- College of Pharmacy. The ^{1}HNMR spectra of the synthesized compounds were measured at 500 MHz, at the central laboratories, Faculty of Sciences, Tehran University, using Varian (Model: Inova). $DMSO_{d6}$ was used as a solvent, and the chemical shifts (δ) expressed in parts per million. Mass spectra were determined using an API 3200 triple quadruple, ESI system (Applied Biosystem). TLC was used to check the progress of reaction, as well as, the purity of products, using solvent system (toluene 75%: ethyl acetae 20%, acetic acid 5%).

Chemical synthesis

Synthesis of ethyl 2-((3-chloro-2-methylphenyl) amino) benzoate (compound 1)[11]:

To 80 mL of abs ethanol, (6g, 0.0229 mol) of tolfenamic acid (TA) were carefully weighed and added. in a 250 mL (RB)-flask, stirred and cooled the liquid to 0 ^{o}C, and then 6 mL of conc. H_2SO_4 was added drop by drop, while stirring continuously. after that, the reaction mixture refluxed at 85 °C with continuous stirring for about 48 h. when reaction completed, the solution was concentrated,

the remaining contents cooled to room temperature, and neutralized with a concentrated solution of $NaHCO_3$, then the aqueous solution extracted with chloroform (3 times × 20 mL). The combined chloroform extracts were dried with anhydrous $MgSO_4$, and the solvent is removed under reduced pressure, powder recrystalized by absolute 70% EtOH yield the corresponding ester. Tolfenamate ethyl ester is a colorless crystal, percent yield (87 %), mp= (65-67 ºC), Rf = 0.91, IR spectra (v, cm^{-1}): 3298 (NH) str, 3080 Ar (CH) str, 2978, 2866 asym and sym str of aliph (CH2 and CH3), 1670 (C=O) str of ester carbonyl, 1581, 1519 Ar (C=C) str,1450 bend of CH3,1248 (C-O) ester str, 744 (C-Cl) str. ^{1}H NMR (500 MHz, DMSOd6, δ=ppm): 9.30 (s, 1H, NH), 7.91 (m, 1H, Ar-H), 7.37 (t, J = 7.9 Hz, 1H, Ar-H), 7.29-7.23 (m, 3H, Ar-H), 6.83-6.77 (m, 2H, Ar-H), 4.33 (q, J = 7.1 Hz, 2H, CH2), 2.25 (s, 3H, Ar-CH3), 1.34 (t, J = 7.1 Hz, 3H, CH3). MS(ESI) m/z: Calcd. for C16H16ClNO2 [M+1]+ 290.09, found 290.30.

Synthesis of 2-((3-chloro-2-methylphenyl)amino)benzohydrazide (compound 2)[12]

An excess of hydrazine hydrate solution 99.9% (2.4 ml ,0.05 mol) and the tolfenamic ethyl ester (3 gm, 0.01 mol) in 100 mL (RB) flask with 50 mL abs.EtOH was set to a reflux at 90 C° for 14h, the colorless solution gradually turned to a faint pink during the reflux. After the finished reflux period, the solution cooled to room temperature, and the solid product was filtered, washed with several portions of EtOH, and dried by suction. Re-crystallization from EtOH afforded the corresponding tolefenamic acid hydrazide. Light-yellow fluffy fine powder, percent yield (78%), mp = (153-155 ºC), R_f= 0.35, IR (v, cm^{-1}): 3329, 3305 (NH_2) str, 3248 (NH)str, 1620 (C=O) str of amide, 1581, 1566, 1508 Ar (C=C) str, 1450 bend of CH_3, 740 (C-Cl) str. ^{1}HNMR (500 MHz, $DMSO_{d6}$, δ=ppm): 9.90 (s, 1H, NH-amide), 9.65 (s, 1H, NH-sec. amine), 7.63 (d, *J* = 7.8 Hz, 1H, Ar-H), 7.31 (t, *J* = 7.8 Hz, 1H, Ar-H), 7.26 (d, *J* = 7.9 Hz, 1H, Ar-H), 7.18 (t, *J* = 8.0 Hz, 1H, Ar-H), 7.13 (d, *J* = 7.9 Hz, 1H, Ar-H), 7.02 (d, *J* = 8.3 Hz, 1H, Ar-H), 6.82 (t, *J* = 7.5 Hz, 1H, Ar-H), 4.55 (s, 2H, NH_2), 2.28 (s, 3H, CH_3). MS(ESI) m/z: Calcd. for $C_{14}H_{14}ClN_3O$ $[M]^+$ 275.08, found 275.40.

Synthesis of 5-(2-((3-chloro-2-methylphenyl)amino)phenyl)-1,3,4-oxadiazole-2-thiol (compound 3)[13]

Compound 2 (2.0 g ,0.007 mol) of was dissolved in 30 mL of abs. EtOH, and KOH (0.407 g ,0.007 mol) was dissolved in 15 mL abs. EtOH, and added to the mixture, and stirred for 15 min. After the mixture was cooled to 0 ºC, 0.85 mL (0.014 mol) of carbon disulfide (CS_2) was added gradually, and a yellow precipitate formed. The reaction was refluxed for 20h, or until the H_2S gas ceased to be produced. After reducing the solvent with a rotary evaporator, and acidifying it with a 10% HCl solution, an off-white precipitate of the product was produced, which recrystallized from EtOH. White to yellow powder, percent yield (75 %), mp = (262-264 ºC), R_f =0.43, IR (v, cm^{-1}): 3340 str of *sec.* amine (NH), 3039, 3028 Ar (C-H) str, 2920 str of (CH_3), 2738 thiol (SH) str, 1616 (C=N) str, 1566, 1500 of Ar (C=C) str, 1450 (CH_3) bend, 1292 (C-O-C) str, 729(C-Cl) str. ^{1}H NMR (500 MHz, $DMSO_{d6}$, δ=ppm): 8.09 (s, 1H, NH), 7.74 (dt, *J* = 7.99, 1.76 Hz, 1H, Ar-H), 7.39 (m, 1H, Ar-H), 7.29-7.25 (m, 3H, Ar-H), 6.95 (t, *J* = 7.57 Hz, 1H, Ar-H), 6.82 (d, *J* = 8.57 Hz, 1H, Ar-H), 2.23 (s, 3H, CH_3). MS(ESI) m/z: Calcd. for

$C_{15}H_{12}ClN_3OS[M+1]^+$ 318.04, found 318.10.

Synthesis of 2-((5-(2-((3-chloro-2-methylphenyl) amino) phenyl)-1,3,4-oxadiazol-2-yl) thio)-1-(4-chlorophenyl) ethan-1-one (compound 4): [14]

Compound (3) (0.7 g, 0.0022 mol) was suspended in 30 mL of abs. EtOH, to which (0.35 mL,0.0044 mol) of triethylamine was added, and stirred for 10 minutes, at room temperature. The suspended mixture transformed into a transparent solution, then carefully added 2-Bromo-4'-chloroacetophenone (0.513 g, 0.0022 mol. The formed precipitate was subsequently filtered, washed with water, and recrystallized from EtOH and DMF to yield the desired compound 4. White crystals, percent yield (88 %), mp = (158-160 ºC), R_f=0.92, IR spectrum (v, cm^{-1}): 3305 (NH) str of *sec.* amine, 2920 (CH_3) str, 1689 (C=O) str, 1608 (C=N) str, 1570, 1546,1504 Ar (C=C) str, 1469 (CH_2) bend, 1431 (CH_3) bend,1276 str of (C-O-C) str, 744 (C-Cl) str. ^{1}H NMR (500 MHz, $DMSO_{d6}$, δ=ppm): 8.85 (s, 1H, NH), 8.09 (dq, *J* = 8.55, 2.34 Hz, 2H, Ar-H), 7.79 (d, *J* = 2.03 Hz, 1H, Ar-H), 7.66 (d, *J* = 2.42 Hz, 2H, Ar-H), 7.38 (t, *J* = 2.06 Hz, 1H, Ar-H), 7.31-7.24 (m, 3H, Ar-H), 6.90 (tt, *J* = 6.67, 2.83 Hz, 2H, Ar-H), 5.19 (s, 2H, CH_2), 2.25 (s, 3H, CH_3). MS(ESI) m/z: Calcd. for $C_{23}H_{17}Cl_2N_3O_2S$ $[M+H]^+$ 470.04, found 470.20.

Synthesis of 2-(2-((3-chloro-2-methylphenyl) amino) benzoyl)-N-(4-chlorophenyl) hydrazine-1-carbothioamide (compound 5): [15]

To a mixture of acid hydrazide (compound **2**) (0.501 g, 0.0018 mol) in 30 mL of abs. EtOH, then we add **4-chlorophenyl isothiocyanate** (0.305 g, 0.0018 mol). The reaction mixture was continuously stirred at 50-55 ºC for 3-4 h, after which the solvent was reduced, cooled, and refrigerated for 10 h. The precipitate was collected, washed with cold EtOH, and recrystallized from 70 % EtOH to produce the final derivative, compound 5. Light yellow fluffy powder, yield (85 %), m.p = (166-168 ºC), R_f =0.55, IR spectra (v, cm^{-1}): 3305 (NH) str of *sec.* amine, 3267 (NH) str of amide, 3159 (NH) str of thioamide, 3059,3035 Ar (CH)str, 2970, 2893 *asym* and *sym* str of (CH_3), 1639 carbonyl(C=O) amide str, 1585, 1527, 1489 Ar (C=C) str, 1454 bend of (CH_3), 1211 (C=S) str, 744 (C-Cl) str. ^{1}H NMR (500 MHz, $DMSO_{d6}$, δ=ppm): 10.63 (s, 1H, NH- thioamide), 9.90 (s, 1H, NH-thioamide), 9.82 (s, 1H, NH of *sec.* amine), 9.66 (s, 1H, NH-amide), 7.89 (d, *J* = 7.9 Hz, 1H, Ar-H), 7.53-7.45 (m, 4H, Ar-H), 7.37 (t, *J* = 7.36 Hz, 1H, Ar-H), 7.27 (d, *J* = 1.90 Hz, 1H, Ar-H), 7.23-7.17 (m, 2H, Ar-H), 7.00 (d, *J* = 8.41 Hz, 1H, Ar-H), 6.85 (t, *J* = 7.55 Hz, 1H, Ar-H), 2.27 (s, 3H, CH_3). MS(ESI) m/z: Calcd. for $C_{21}H_{18}Cl_2N_4OS$ $[M+H]^+$ 445.06, found 445.30.

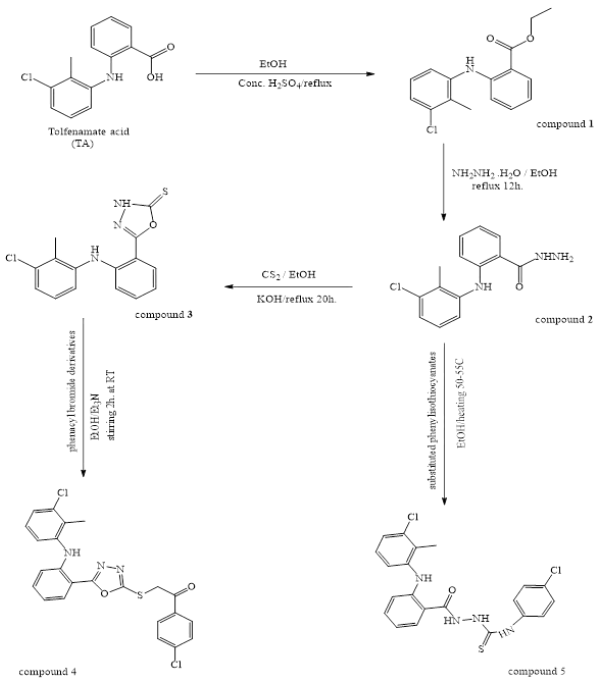

Scheme 1. Chemical synthesis of the new tolfenamic acid (TA) derivatives

Molecular docking studies
Method of docking process

After completing the pharmacophore study and selecting the target protein, the MOE 19.0901 software should have been used to determine the modes of molecular binding for the tested chemical within the pockets of (VEGFR tyrosine kinase). The co-crystallized ligand was used to generate the binding sites within the crystal protein (PDB codes: 4ASD) (https://www.rcsb.org). Initially, water molecules were eliminated from the complex. Then, using protein report, utility, and clean protein options, crystallographic disorders and unfilled valence atoms were corrected. MMFF94 force fields were used to reduce protein energy. The protein structure with a rigid binding site was created using a fixed atom constraint. Identifying and preparing the protein's necessary amino acids needed for docking. , the saved file(2D structure of tested compound) was opened, In MOE 19.0901 Software, 3D structures were protonated, and energy was reduced by applying 0.05 RMSD kcal/mol. MMFF94 force field[16]. When this procedure was completed, the docked structures were prepared utilizing the ligand preparation technique. The CDOCKER protocol was used to perform molecular docking. For refinement, the receptor was kept rigid while the ligands were allowed to be flexible. This allowed each molecule to interact with the protein in ten various ways[17]. Using Discovery Studio 2019 Client, the docking scores (-CDOCKER interaction energy) were recorded, and 3D views were created for the best fitted poses that suit the active site at the (VEGFR tyrosine kinase). Preliminary calculations are made for each docking position, and the binding Free Energy (ΔG) of the investigated compounds, with (VEGFR tyrosine kinase).

Validation of molecular docking

The reliability and reproducibility of the suggested docking procedure were first tested by redocking the corystallized ligand into the active site of the relevant receptor, and calculating the root mean square deviation (RMSD). The docking of a co-crystallized ligand to the crystallographic structure of VEGFR (4ASD), resulted in an RMSD of 1.36, less than 2.00 A° showing that the algorithm used was verified against the crystallographic structure [18].

Results and Discussion

Chemistry

Compound (1), (ethyl 2-(3-chloro-2-methylphenyl) amino) benzoate was synthesized by treating tolfenamic acid with ethanol using conc. H_2SO_4, then it was exposed to aminolysis with hydrazine hydrate to generate compound 2, which reacted with CS_2 in ethanolic KOH solution to afford oxadiazole, compound 3. The intermediate 3 was reacted with substituted phenacylbromide derivative yield the final compound 4. Whereas compound 2 was reacted with substituted phenylisothiocyanate to yield the desired compounds 5 bearing the hydrazine-1-carbothioamide moiety. The IR spectrum for compound 2 showed a band at 3329 and 3305 cm^{-1} as doublet for NH_2 stretching. While for compound 3 an absorption bands at 2738 cm^{-1} for SH stretching, and at 1616 and 1566 cm^{-1} for (C=N) stretching. For the titled compound 4, the IR spectrum revealed a characteristic absorption bands at 1689 cm^{-1} for carbonyl (C=O) stretching, and at 1278 cm^{-1} specific for (C-O-C) stretching. The IR spectrum of the hit compound 5 revealed characteristic absorption bands at 3159 cm^{-1} for NH stretching of the thioamide moiety, and a band at 1211 cm^{-1} for (C=S) stretching. The ^{1}H-NMR signal assignments of protons revealed the formation of the desired products. For compound 4, The new signals that appeared at δ= 5.19 ppm value was attributed to *aliph.*CH_2 group. Compound 5 spectra revealed new signals at δ= 10.63 ppm assigned to distinct NH protons of the thioamide moiety. The success of the synthesis of the final compounds with their intermediate was further confirmed by their mass spectra.

Docking study

Generation of 3D-pharmacophore model

The primary goal of pharmacophore-based drug design is to construct a three-dimensional pharmacophore model using the established receptor-ligand pharmacophore generating method. In this approach, various features would be expected from the study of the binding of the ligand with the target protein. These features are essential for the activity. Consequently, any ligand that contains these features is expected to be active. A process of 3D-pharmacophore generation was validated and resulted in a 3D pharmacophore model consisting of four features shown in (Figure 1). The generated model was used to examine the tested compounds as possible ligands for VEGFR-2 TK [19].

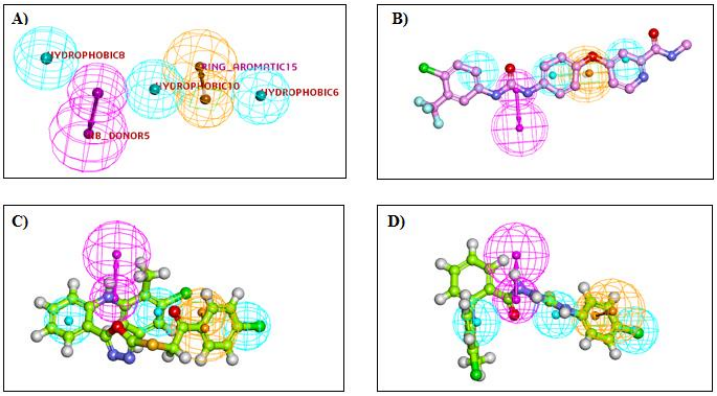

Figure 1. A) The produced 3D-pharmacophore geometry has four criteria; Aromatic ring (blue), linker with hydrophobic aromatic ring (orang) hydrogen bond donor and acceptor center (violet), and terminal aromatic ring (blue). B-D) Mapping of the different compounds on the generated pharmacophore. B) Sorafenib (Fit value = 3.233); C) Ligand 4 (Fit value = 3.093); D) Ligand 5 (Fit value = 3.309)

Activity prediction

The synthetic (TA) ligands, and crystal ligands were tested against the 3D-pharmacophore model that had been constructed. Fit values between the tested ligand and the created 3D-pharmacophore were generated in this method (which quantitatively represents the existence of those key properties). All the (TA) ligands were found to contain all the critical features of the VEGFR-2 TK inhibitor (Table 1).

Table 1
Essential features, fit values and relative fit of the tested fenamate ligands, and sorafenib based on the generated pharmacophore model

Ligand	Pharmacophoric queries	Pharmacophore-Fit score
Sorafenib	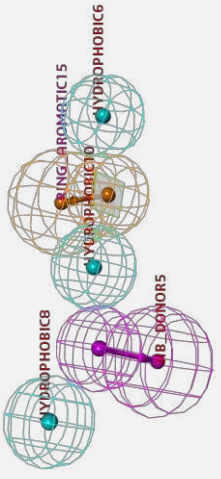	3.233
		3.093
		3.309

Docking study

Table 2 showed binding free energy (ΔG, docking score kcal/mol) of synthesized compounds against VEGFR-2 tyrosine kinase target site PDB ID: 4ASD. The crystal ligand (sorafenib) binding mode revealed an energy binding of -8.50 kcal/ mol^{-1} against VEGFR tyrosine kinase. The N-methyl picolinamide moiety formed five *pi-pi, pi*-sulfur, and *pi*-alkyl interactions with Ala866, Leu840, Leu1035, Phe918 and one H-bond with Cys919, as well as, the 4-chloro-3-(trifluoromethyl)phenyl)ureido)phenoxy moiety interact with Asp1046, Glu885 and Val899 by four H-bonds, moreover, fourteen *pi*-alkyl and *pi*-sulfur interactions with Val916, Lys868, Cys1045, Val848, Val899, Ala866, Leu1019, Ile892 , Leu889,Ile888 and two halogen interactions with Ile1044 (Figure 2).

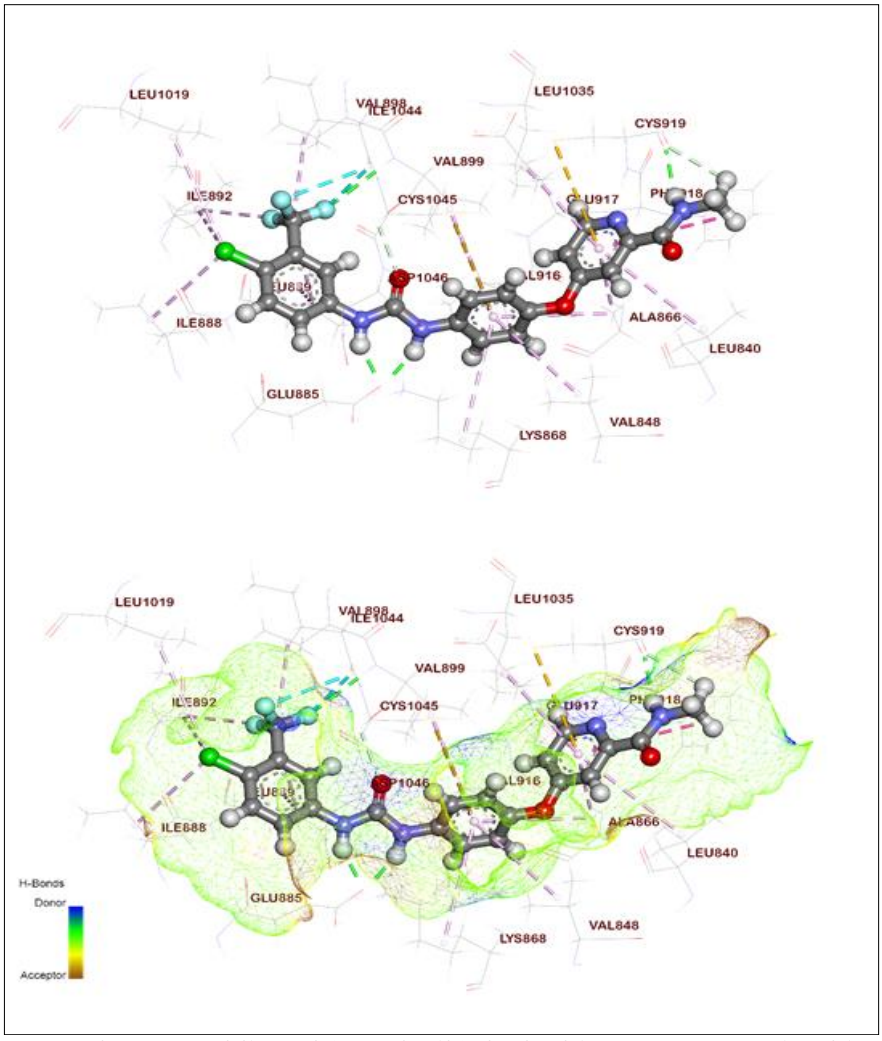

Figure 2. The Crystal ligand (Sorafenib) docked in VEGFR tyrosine kinase, hydrogen bonds (green) and the *pi* interactions are represented in purple lines with Mapping surface showing the crystal ligand occupying the active pocket of VEGFR tyrosine kinase

The candidate compound 4 displayed binding interaction of -8.78 kcal/ mol against VEGFR-2 tyrosine kinase. The (3-chloro-2-methylphenyl) amino) phenyl) moiety generated fourteen *pi*-alkyl, *pi-pi,* and *pi*-anion interactions with Lys868, Val914, Val916, Val848, Phe1047, Leu1035, Ala866, Leu840, Cys1045, and Val899, and it interacted with Asp1046 by one H-bond (2.20 ºA). In addition, 1,3,4-oxadiazol-2-yl) thio)-1-(4-chlorophenyl) ethan-1 moiety interacted with Arg1027, His1026, Asp814, Leu889, Cys1045, Lys868 to form seven *pi-pi*, *pi*-cation, *pi*-alkyl, and *pi*-anion interactions (Figure. 3).

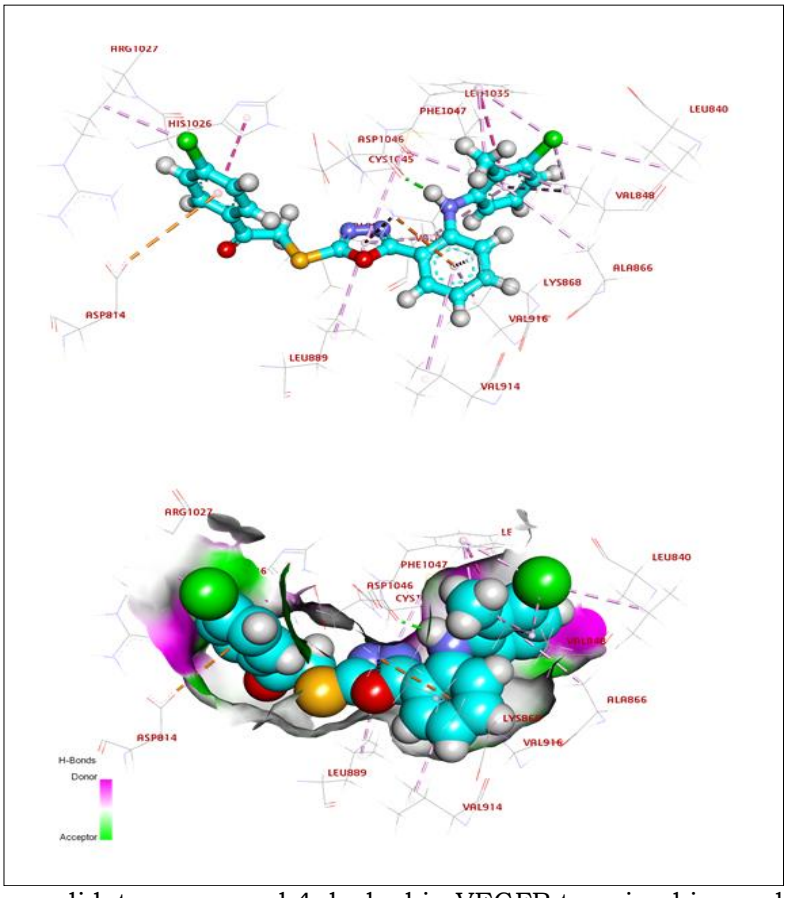

Figure 3. candidate compound 4 docked in VEGFR tyrosine kinase, hydrogen bonds (green) and the *pi* interactions are represented in purple lines

The hit compound 5 generated an energy of interaction of -8.91 kcal/ mol against VEGFR-2 tyrosine kinase. The (3-chloro-2-methylphenyl) amino) benzoyl) moiety generated five *pi* -alkyl, *pi*-cation, and *pi*-anion interactions with Leu889, Ile888, Asp814, Arg1027, and Asp1046. The (4-chlorophenyl) hydrazine-1-carbothioamide interacted with Asp1046 by one H-bond, with a distance of 2.19 ºA. Additionally, nine *pi*-alkyl and *pi-pi* interactions were formed with Leu840, Phe1047, Cys1045, Val899, Val848, Leu1035 and Ala866 (Figure 4).

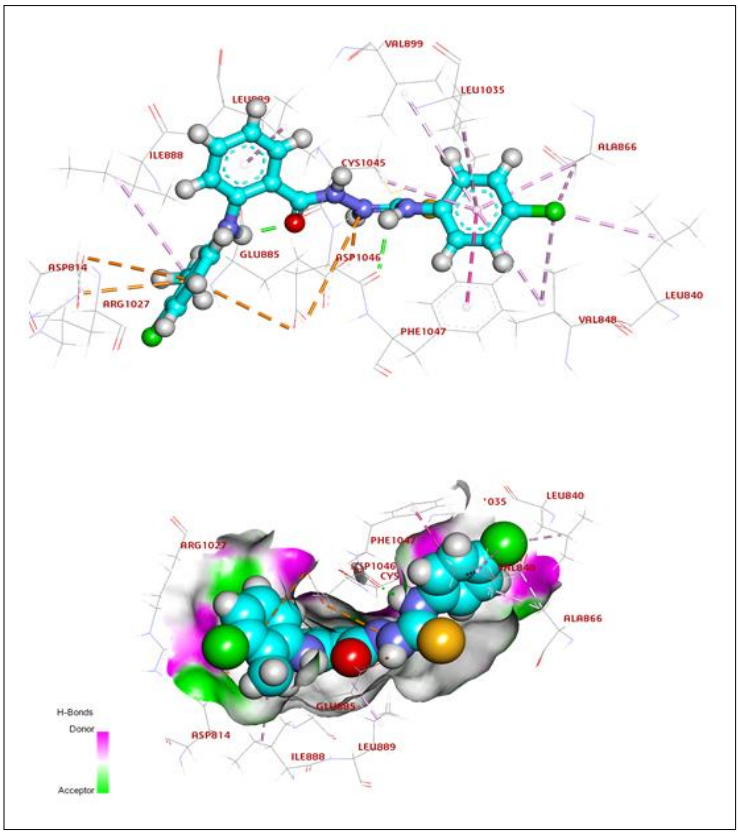

Figure 4. candidate compound 5 docked in VEGFR tyrosine kinase, hydrogen bonds (green) and the pi interactions are represented in purple lines

Table 2
Binding free energy (ΔG, docking score kcal/mol) of the synthesized fenamate compounds against VEGFR-2 tyrosine kinase target site PDB ID: 4ASD

Ligand	RMSD value (Å)	Docking score (kcal/mol)	Interactions	
			H.B	pi-interactions
Sorafenib	1.36	-8.50	5	17
Compound 4	1.08	-8.78	1	21
Compound 5	1.57	-8.91	1	14

Molecular Similarity study

Molecular similarity is a ligand-based computer technique used to predict the similarity between two compounds. This work is predicated on the idea that structurally identical ligands will have comparable characteristics to various molecules. Calculating molecular similarity focuses on the molecular attributes of the investigated ligands, such as log p, and molecular weight. In addition, the majority of the molecular similarity is determined by the spatial distances between structural and physicochemical parameters. Six ligands with anticancer

activity against (VEGFR-2 TK crystal ligand) were subjected to a molecular similarity study utilizing Discovery Studio software. Table 3 shows some of the molecular features that are employed: the number of rotatable bonds, cyclic rings, aromatic rings, hydrogen bond donors (HBD), hydrogen bond acceptors, partition coefficient (log p), molecular weight (M. Wt), and molecular fractional polar surface area (MFPSA) [20].

Table 3
(TA) ligands with crystal ligands and their molecular properties

Comp.	Log p	M. Wt	HBA	HBD	Rotatable bonds	Rings	Aromatic rings	MFPSA	Is similar
4	6.833	470.371	5	1	7	4	4	0.212	similar
5	6.639	445.365	3	4	7	3	3	0.233	similar
Sorafenib	4.175	464.825	4	3	6	3	3	0.212	Reference

ADMET studies

Sorafenib was used as a reference drug in the assessment of six ADMET criteria using Discovery Studio software. Blood penetration levels (BBB) of all ligands were found to be medium to low, indicating less potential for central nervous system (CNS) negative effects [21]. The solubility of all ligands was between medium and low. Furthermore, all of the evaluated ligands were found to be non-inhibitors of cytochrome p450, and they were well absorbed. All the ligands were anticipated to be non-hepatotoxic. However, sorafenib had some degrees of *in silico* hepatotoxicity. Lastly, some ligands were expected to bind plasma protein (PPB) by more than 90% [22, 23]. As a result of these findings, all ligands were chosen for further studies because of their excellent pharmacokinetic qualities, Table 4.

Table 4
ADMET properties anticipated for the newly created compounds

Comp.	BBB level a	Solubility level b	Absorption level c	Hepatotoxicity	CYP2D6 prediction D	PPB prediction e
4	4	1	2	*True*	*False*	*true*
5	4	1	1	*True*	*False*	*true*
Sorafenib	4	1	0	*True*	*False*	*true*

a BBB level, blood brain barrier level, 0 = very high, 1 = high, 2 = medium, 3 = low, 4 = very low. b Solubility level, 1 = very low, 2 = low, 3 = good, 4 = optimal. c Absorption level, 0 = good, 1 = moderate, 2 = poor, 3 = very poor. d CYP2D6,

cytochrome P2D6, TRUE = inhibitor, FALSE = non inhibitor. The classification of whether a compound is a CYP2D6 inhibitor using the cutoff Bayesian score of 0.161. e PBB, plasma protein binding, FALSE means less than 90%, TRUE means more than 90%. The classification of whether a compound is highly bounded (≥ 90% bound) to plasma proteins using the cutoff Bayesian score of -2.209.

Toxicity studies

Using the reference molecule sorafenib and the software Discovery Studio, virtual toxicity tests against several toxicity models have been conducted. The outcome is summarized in Table 5.

Table 5
The toxicity properties of the newly synthesized compounds *in silico*

	FDA Rodent Carcinogenicity (Male, mouse)	Carcinogenic Potency TD50 (Rat) [a]	Rat Maximum Tolerated Dose (Feed) [b]	Developmental Toxicity Potential	Rat Oral LD50[b]	Rat Chronic LOAEL[b]	Ocular Irritancy (Rat)	Ski Irrit (Rat
	Non-Carcinogen	5.032	0.109	Non-Toxic	0.37	0.025	Mild	Non Irrit
	Non-Carcinogen	15.52	0.408	Non-Toxic	3.14	0.23	Mild	Non Irrit
i	Non-Carcinogen	14.24	0.088	Maybe Toxic	0.822	0.004	Mild	Non Irrit

[a] Unit: mg/kg body weight/day. [b] Unit: g/kg body weight.

DFT study

Some synthesized ligands 4 and 5 were chosen for DFT studies to investigate their electronic profile. Discovery Studio software was utilized in this test. Crystal ligand sorafenib were utilized as a reference molecule. The calculated DFT parameters include total energy of the molecules, binding energy, energy of the highest occupied molecular orbital (HOMO), the energy of the lowest unoccupied molecular orbital (LUMO), and the magnitude of the dipole moment (μ)as illustrated in (Figure 5). The HOMO is coupled with an electron donor ability, while LUMO is linked to the acceptance of electrons. These orbitals describe the way the ligand will interact with other species. The gap energy helps to expect the chemical reactivity with kinetic stability of a drug. Furthermore, the total dipole moment describes the ability of interaction of a chemical candidate with the surrounding environment [24]. The results of DFT studies were summarized in Table 6.

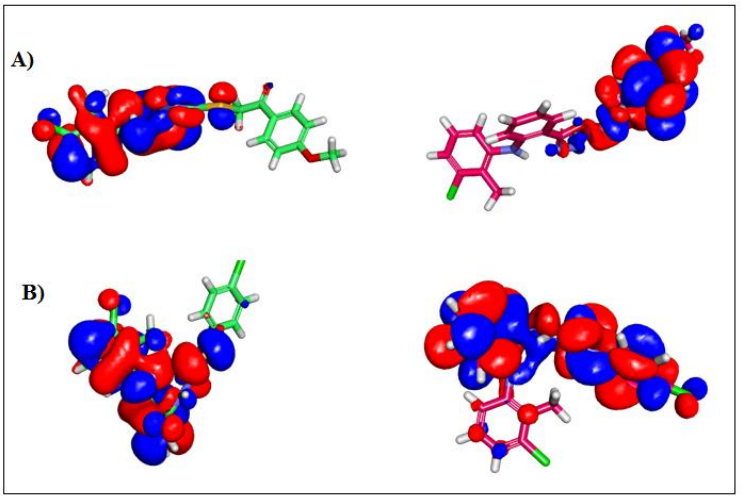

Figure 5. Spatial distribution of molecular orbitals for A) Ligand 4; B) Ligand 5.

Table 6
Spatial distribution of molecular orbitals for the tested ligands

Comp.	Total Energy (kcal/mol)	Binding Energy (kcal/mol)	HOMO Energy (kcal/mol)	LUMO Energy (kcal/mol)	Dipole Mag(debye)	Band Gap Energy
4	-2505.19	-9.8720	-0.187	-0.113	0.906	0.074
5	-2409.93	-9.4610	-0.193	-0.083	2.405	0.110

3D-QSAR model generation and validation

A training set of 32 FDA approved VEGFR -2 inhibitors of known activity with IC_{50} values ranging from 0.035 to 1.2 μM were collected from the Selleckchem library

The structures of the training set of FDA approved selective VEGFR-2 inhibitors were first drawn using ChemBioDraw Ultra 17.0, and saved in MDL-SD file format. The saved file was then opened with Discovery Studio 2016 [30]. Using the Ligand Prepare protocol, the structures were prepared, and the force fields (CHARMM and MMFF94) were applied. After ligand preparation, 3D-QSAR model was generated by the GridBasedTempModel protocol (Supplementary Table 1 and 2). Using GridBasedTempModel analysis, quantitative structure–activity relationship (QSAR) investigations were conducted to determine the effect of substituents on anticancer activity. A training set of 32 FDA-approved VEGFR-2 inhibitors was subjected to GBTM analysis for model creation in the present study. The data on anti-cancer activity was converted from IC_{50} to PIC_{50} (i.e., -logIC_{50}), and used as dependent variables in the QSAR analyses (supplementary Table 3).

The generated QSAR model was represented graphically by scattering plots of the predicted anti-cancer activity against VEGFR-2 versus the experimental values for the training set compounds, as shown in (Figure 6). Also, Table 7 shows how the

predicted anticancer activity of the synthesized compounds against VEGFR-2 was tested, and how the QSAR model predicted it would be.

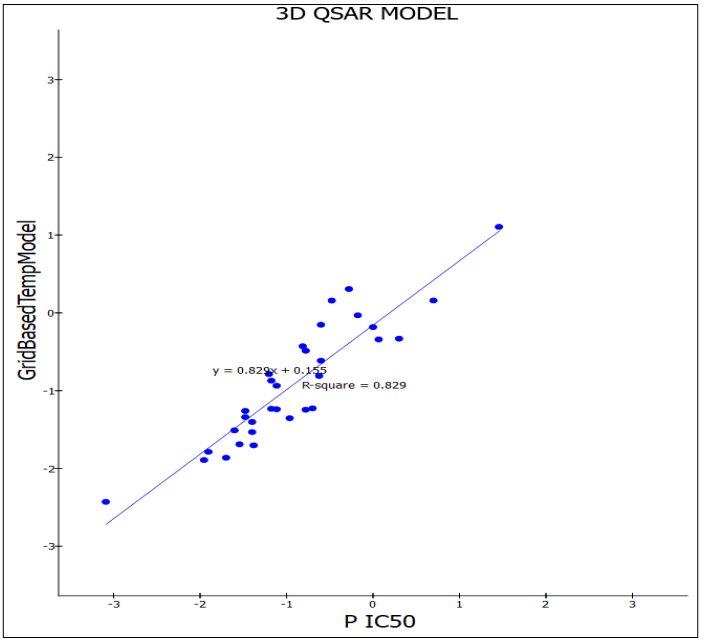

Figure 6. Predicted (Y axis) versus experimental anticancer activity (X axis -PIC_{50}) of the training set compounds against VEGFR-2 target site.

Table 7
The IC_{50}- of the newly fenamate-derivatives against VEGFR-2

Compound	IC_{50}(nM)
4	91.20
5	57.40
Sorafenib	90

SAR study

A study of the structure-activity relationship (SAR) of the novel compounds identified a bunch of common outcomes. The presence of an aryl or a heteroaryl fragment attached with the hydrophilic linker is crucial to the anticancer activity. Accordingly, compounds that have a hydrazine-1-carbothioamide moiety showed good activity (IC_{50} = 57.40 nM) compared with those containing an oxadiazole moiety (IC_{50} = 91.20 nM), as stated in (Figure 7).

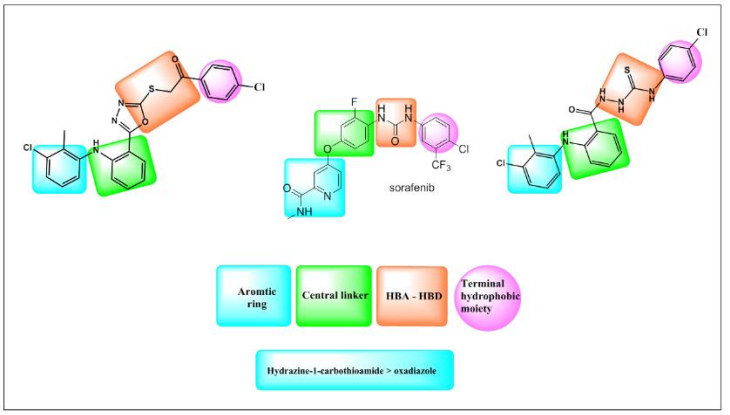

Figure 7. The structure-activity relationship (SAR) of the new compounds, and sorafenib revealed several common features

Conclusion

The current work presented the design and synthesis of two new compounds (hydrazine-1-carbothioamide and 1,3,4-oxadiazol-2-thione) tolfenamic acid derivatives, were synthesized and analyzed using a variety of spectral techniques. All the purified compounds were tested for in *silico* VEGFR-2 tyrosine kinase inhibitory activity, and that compound 4 and 5, predicted IC_{50} concentration (91.20 and 57.40 nM) respectively is very close to that of the standard VEGFR tyrosine kinase inhibitor sorafenib (90 nM), suggested that these compounds a very promising VEGFR-2 tyrosine kinase (upregulated in solid tumors) antagonist.

Acknowledgment

The authors gratefully acknowledge the Dept. of Pharmaceutical Chemistry, College of Pharmacy, University of Baghdad for providing facilities for the current work.

Conflict of interest

No conflict of interest was found or declared by any of the authors.

Funding

This study received no funding from any agency at any point in its development.

References

Abbas, A. H., Mahmood, A. A. R., Tahtamouni, L. H., Al-Mazaydeh, Z. A., Rammaha, M. S., Alsoubani, F., & Al-bayati, R. I. New picolinic acid derivatives: Synthesis, docking study and anti-EGFR kinase inhibitory effect. Mater Today Proc. Published online. 2021. https://doi.org/10.1016/j.matpr.2021.05.354.

Abdelrehim ESM. Synthesis and Screening of New [1,3,4]Oxadiazole, [1,2,4]Triazole, and [1,2,4]Triazolo[4,3- b][1,2,4]triazole Derivatives as Potential

Antitumor Agents on the Colon Carcinoma Cell Line (HCT-116). ACS Omega. 6(2) (2021) 1687-1696. https://doi.org/10.1021/acsomega.0c05718.

Aboul-Fadl, T.; Abdel-Aziz, H.A.; Kadi, A.; Bari, A.; Ahmad, P.; Al-Samani, T.; Ng, S.W. Microwave-assisted one-step synthesis of fenamic acid hydrazides from the corresponding acids. Molecules.16(5) (2011) 3544-3551. https://doi.org/10.3390/molecules16053544.

Ahmed WS, Razzak Mahmood Kubba AA, Al-Bayati RI. Synthesis and evaluation of antimicrobial activity of new imides and schiff bases derived from Ethyl-4-Amino Benzoate. Orient J Chem. 34(5) (2018) 2477-2486. http://dx.doi.org/10.13005/ojc/340533.

Alanazi, M. M., Elwan, A., Alsaif, N. A., Obaidullah, A. J., Alkahtani, H. M., Al-Mehizia, A. A., Alsubaie, S. M., Taghour, M. S., & Eissa, I. H. Discovery of new 3-methylquinoxalines as potential anti-cancer agents and apoptosis inducers targeting VEGFR-2: Design, synthesis, and in silico studies. J Enzyme Inhib Med Chem. 36(1) (2021) 1732-1750. https://doi.org/10.1080/14756366.2021.1945591.

Alanazi, M. M., Mahdy, H. A., Alsaif, N. A., Obaidullah, A. J., Alkahtani, H. M., Al-Mehizia, A. A., Alsubaie, S. M., Dahab, M. A., & Eissa, I. H. New bis ([1, 2, 4] triazolo)[4, 3-a: 3′, 4′-c] quinoxaline derivatives as VEGFR-2 inhibitors and apoptosis inducers: design, synthesis, in silico studies, and anticancer evaluation. Bioorg Chem.112 (2021) 104949. https://doi.org/10.1016/j.bioorg.2021.104949.

Al-Bayati, A. I., Razzak Mahmood, A. A., Al-Mazaydeh, Z. A., Rammaha, M. S., Al-bayati, R. I., Alsoubani, F., & Tahtamouni, L. H. Synthesis, Docking Study, and in Vitro Anticancer Evaluation of New Flufenamic Acid Derivatives. Pharmacia. 68(2) (2021) 449-461. https://doi.org/10.3897/pharmacia.68.e66788.

Alsaad H, Kubba A, Tahtamouni LH, Hamzah AH. Synthesis , docking study , and structure activity relationship of novel anti-tumor 2- (2 , 3- dimethyl aminobenzoic acid) moiety. Pharmacia. 69(2) (2022) 415-428.. https://doi:10.3897/pharmacia.69.e83158.

Amir M, Shikha K. Synthesis and anti-inflammatory, analgesic, ulcerogenic and lipid peroxidation activities of some new 2-[(2,6-dichloroanilino) phenyl]acetic acid derivatives. Eur J Med Chem. 39(6) (2004) 535-545. https://doi.org/10.1016/j.ejmech.2004.02.008.

Aziz, M. A., Serya, R. A. T., Lasheen, D. S., Abdel-Aziz, A. K., Esmat, A., Mansour, A. M., Singab, A. N. B., & Abouzid, K. A. M. Discovery of potent VEGFR-2 inhibitors based on furopyrimidine and thienopyrimidne scaffolds as cancer targeting agents. Sci Rep. 6(1) (2016) 1-20. https://doi.org/10.1038/srep24460.

Coutsias EA, Seok C, Dill KA. Using quaternions to calculate RMSD. J Comput Chem. 25(15) 2(004) 1849-1857. https://doi.org/10.1002/jcc.20110.

Davoud Ahmadvand, PhD, Fatemeh Rahbarizadeh, PhD, Farnoush Jafari Iri-Sofla, PhD student, Gholamreza Namazi, PhD student, Sepideh Khaleghi, MSc, Bita Geramizadeh, PhD, Parvin Pasalar, PhD, Hosein Karimi, PhD, Seyed Hamid Aghaee Bakhtiari, PhD student. Inhibition of angiogenesis by recombinant VEGF receptor fragments. Lab Med. 41(7) (2010) 417-422. https://doi.org/10.1309/LMMH2WYRLP7B3HJN.

El-Adl, K., Sakr, H. M., Yousef, R. G., Mehany, A. B. M., Metwaly, A. M.,

Elhendawy, M. A., Radwan, M. M., ElSohly, M. A., Abulkhair, H. S., & Eissa, I. H. Discovery of new quinoxaline-2 (1H)-one-based anticancer agents targeting VEGFR-2 as inhibitors: Design, synthesis, and anti-proliferative evaluation. Bioorg Chem. 114 (2021) 105105. https://doi.org/10.1016/j.bioorg.2021.105105.

El-Helby AA, Sakr H, Eissa IH, Abulkhair H, Al-Karmalawy AA, El-Adl K. Design, synthesis, molecular docking, and anticancer activity of benzoxazole derivatives as VEGFR-2 inhibitors. Arch Pharm (Weinheim). 352(10) (2019)1900113. https://doi.org/10.1002/ardp.201900113.

Hmood, K. S., & Razzak Mahmood Kubba, A. A. Synthesis, docking study and in Vitro anticancer evaluation of new derivatives of 2-(1-(2-flouro-[1,1-biphenyl]-4-Yl)Ethyl)-6-(Substituted Phenyl) imidazole[2,1-B][1,3,4]thiadiazole derived from flurbiprofen. Systematic Reviews in Pharmacy, 12(2) (2020) 184–201. https://doi.org/10.31838/srp.2021.2.24.

Kardina, I., Ramadany, S., Sanusi B, Y., Made, S., Stang, S., & Syarif, S. (2020). Children's midwifery learning media application about android-based rough motor development in improving midwifery student skills. International Journal of Health & Medical Sciences, 3(1), 146-152. https://doi.org/10.31295/ijhms.v3n1.300

Lemmon MA, Schlessinger J. Cell signaling by receptor tyrosine kinases. Cell. 141(7) (2010) 1117-1134. https://doi.org/10.1016/j.cell.2010.06.011.

Lugano R, Ramachandran M, Dimberg A. Tumor angiogenesis: causes, consequences, challenges and opportunities. Cell Mol Life Sci. 77(9) (2020) 1745-1770. https://doi:10.1007/s00018-019-03351-7.

Maiti P., Sharma, P., Nand, M., Bhatt, I. D., Ramakrishnan, M. A., Mathpal, S., Joshi, T., Pant, R., Mahmud, S., & Simal-Gandara, J. Integrated Machine Learning and Chemoinformatics-Based Screening of Mycotic Compounds against Kinesin Spindle ProteinEg5 for Lung Cancer Therapy. Molecules. 27(5) (2022) 1639. https://doi.org/10.3390/molecules27051639.

Modi SJ, Kulkarni VM. Vascular Endothelial Growth Factor Receptor (VEGFR-2)/KDR Inhibitors: Medicinal Chemistry Perspective. Med Drug Discov. 2 (2019) 100009. https://doi.org/10.1016/j.medidd.2019.100009.

Nara, Sukanya Garlapati A. Design, Synthesis and molecular docking study of hybrids of quinazolin-4(3H)-one as anticancer agents TT - Diseño, síntesis y estudio de acoplamiento molecular de híbridos de quinazolinona-tiazolidin-4-onas como agentes anticancerígenos. Ars Pharm. 59(3) (2018) 121-131. http://dx.doi.org/10.1016/j.bmcl.2016.08.013.

Nawaf A. Alsaif, Mohammed S. Taghour, Mohammed M. Alanazi, Ahmad J. Obaidullah, Abdulrahman A. Al-Mehizia, Manal M. Alanazi, Saleh Aldawas, Alaa Elwan & Hazem Elkady. Discovery of new VEGFR-2 inhibitors based on bis ([1, 2, 4] triazolo)[4, 3-a: 3', 4'-c] quinoxaline derivatives as anticancer agents and apoptosis inducers. J Enzyme Inhib Med Chem. 36(1) (2021) 1093-1114. https://doi.org/10.1080/14756366.2021.1915303.

Rizkiyati, I., Ahmad, M., Syarif, S., & Ahmar, H. (2021). Analysis of motivation and behavior of midwives in using digital partographs. International Journal of Life Sciences, 5(2), 48–58. https://doi.org/10.29332/ijls.v5n2.1234

Sana, S., Reddy, V. G., Bhandari, S., Reddy, T. S., Tokala, R., Sakla, A. P., Bhargava, S. K., & Shankaraiah, N. Exploration of carbamide derived pyrimidine-thioindole conjugates as potential VEGFR-2 inhibitors with anti-angiogenesis effect. Eur J Med Chem. 200 (2020) 112457.

https://doi.org/10.1016/j.ejmech.2020.112457.
Suryasa, I. W., Rodríguez-Gámez, M., & Koldoris, T. (2021). The COVID-19 pandemic. International Journal of Health Sciences, 5(2), vi-ix. https://doi.org/10.53730/ijhs.v5n2.2937
Zhang Y, Zou JY, Wang Z, Wang Y. Fruquintinib: a novel antivascular endothelial growth factor receptor tyrosine kinase inhibitor for the treatment of metastatic colorectal cancer. Cancer Manag Res. 11 (2019) 7787-7803. https://doi:10.2147/CMAR.S215533.
Zirlik, K., & Duyster, J.. Anti-angiogenics: current situation and future perspectives. Oncology Research and Treatment. 41(4) (2018)166–171. https://doi.org/10.1159/000488087.

Supplementary data

Supplementary Table 1. Validity of our QSAR model was proven by Leave-one-out (LOO) internal validation (r 2 = 0.829). Cross-validation was also employed where q 2, which is equivalent to r 2 (pred), was 0.829. The increased value of q 2 over than 0.5 reveals the validity of a QSAR model. Moreover, measuring the residuals between the experimental and the predicted activities of the training set gave an additional QSAR model validation, where the predicted activities by the established QSAR model were very close to those experimentally assessed, indicating that this model could be applied for anti-cancer prediction of other effective analogues

Suppl. table 1. 5-Fold Cross Validation Result

Number of Components	q2	RMS Error	Mean Absolute Error
1	0.009	0.870	0.645
2	0.002	0.870	0.643
3	0.006	0.862	0.632
4	0.006	0.862	0.633
5	0.007	0.861	0.632
6	0.007	0.861	0.632

Supplementary Table 2. Validation of the results using external test set VEGFR-2_model

Model Name	q^2	RMS Error	Mean Absolute Error
Grid BasedTemp Model	0.829	0.350	0.291

Supplementary Table 3.

Comparision of experimental and predicted anticancer activity of training set of compounds against VEGFR-2 obtained by QSAR model

Compound	Experimental PIC_{50}	Predicted PIC_{50}	Residual
FDA VEGFR-2	1.45593	1.10496	0.35097
	0	-0.184	0.184
	-0.176	-0.031	-0.140

proved drugs	-0.272	0.3061	-0.586
	-0.778	-1.245	0.467
	-0.963	-1.354	0.390
	-1.176	-0.872	-0.303
	-1.204	-0.787	-0.416
	-1.477	-1.261	-0.216
	-1.903	-1.786	-0.115
	-3.089	-2.429	-0.659
	0.698	0.1583	0.540
	0.3010	-0.332	0.633
	0.065	-0.342	0.407
	-0.477	0.1574	-0.636
	-0.602	-0.615	0.013
	-0.602	-0.153	-0.448
	-0.623	-0.811	0.188
	-0.698	-1.227	0.528
	-0.778	-0.487	-0.291
	-0.812	-0.429	-0.383
	-1.113	-1.239	0.125
	-1.113	-0.93	-0.176
	-1.176	-1.239	0.057
	-1.380	-1.703	0.323
	-1.397	-1.532	0.135
	-1.397	-1.403	0.0052
	-1.477	-1.340	-0.136
	-1.544	-1.690	0.146
	-1.602	-1.511	-0.090
	-1.698	-1.863	0.164
	-1.954	-1.893	-0.061